Evidence for Barotropic Wave Radiation from the Gulf Stream*

AMY S. BOWER AND NELSON G. HOGG

Woods Hole Oceanographic Institution, Woods Hole, Massachusetts

(Manuscript received 26 November 1990, in final form 24 May 1991)

ABSTRACT

Highly energetic velocity fluctuations associated with topographic Rossby waves are frequently observed over the continental slope and rise off the United States and Canadian east coast. It has been suggested that the energy source for these waves could be eastward-propagating Gulf Stream meanders, which can couple to the westward-propagating Rossby waves if the meander shape is time dependent. In this study, a historical archive of all available current meter data from the western North Atlantic has been examined for evidence of energy radiation from the Gulf Stream via barotropic/topographic Rossby waves. Maps of abyssal eddy kinetic energy (EKE) and Reynolds stress were constructed for four frequency bands (including motions with periods between 256 and 7.8 days) to examine distributions of these quantities over the largest possible geographical area.

Maximum eddy kinetic energy is observed along the mean axis of the Gulf Stream at low frequencies (50–250 days), but this maximum shifts north and west with increasing frequency. The westward shift may be due to the fact that the phase speed of Gulf Stream meanders decreases with increasing downstream distance. The northward shift of maximum EKE to a position over the continental slope and rise is discussed in terms of the refraction and convergence of barotropic Rossby wave energy rays emanating from the region of the Gulf Stream.

The Reynolds stress maps show strong evidence of onshore energy radiation north of the Gulf Stream over a large geographical area and at all frequencies considered. The velocity components are found to be statistically coherent and 180° out of phase at many locations when viewed in a coordinate system aligned with the local ambient potential vorticity gradient. Energy radiation away from the Stream to the south, although expected, is not apparent in the observations, perhaps due to the dominance of other eddy-generating mechanisms there such as baroclinic instability of the westward recirculation.

Large-scale features of the maps compare poorly with similar maps generated from a stochastic wave radiation model, and it is suggested that such models need to include more realistic forcing and basin geometry before detailed model–data comparisons can be made.

1. Introduction

During the past two decades, direct observations of the deep velocity fluctuations in the North Atlantic have revealed that the distribution of eddy kinetic energy (EKE) is anything but uniform over the basin. Schmitz (1984) assembled all available estimates of EKE from current meter records at 4000 m and clearly illustrated that the highest values of abyssal EKE are found in the western North Atlantic, particularly in the vicinity of the Gulf Stream downstream of Cape Hatteras. Maximum EKE levels (>100 cm^2 s^{-2}) were observed along the mean axis of the Gulf Stream, most likely due to the energetic meanders in the path of the current that grow to large amplitude in this area. However, significant EKE levels (>10 cm^2 s^{-2}) extend outward for considerable distances to the north and south, well beyond the direct influence of the meandering [compare Schmitz's (1984) Fig. 5 with Cornillon's (1986) Fig. 2].

Several mechanisms have been suggested that could generate the pool of relatively high eddy energy in the deep western North Atlantic. One possibility is the release of available potential energy stored in the interior mean Sverdrup circulation through baroclinic instability (Gill et al. 1974; Hogg 1985). The reflection of westward-propagating planetary Rossby waves at the U.S. continental margin is another possibility (Pedlosky 1979). In this study, we will consider a third mechanism, namely, barotropic Rossby wave radiation from the Gulf Stream.

The motivation for considering this mechanism arises from the increasing number of observations of highly energetic planetary and topographic Rossby waves in the vicinity of the Gulf Stream. For example, Thompson (1977) identified the low-frequency motions on the continental rise south of New England as topographic Rossby waves. He observed that the velocity fluctuations produced a significant negative Reynolds stress ($\overline{u'v'} < 0$) and suggested that the energy source

* Woods Hole Oceanographic Institution Contribution No. 7587.

Corresponding author address: Dr. Amy Bower, Woods Hole Oceanographic Institute, Clarke Laboratory, Woods Hole, MA 02543.

for the wave motions lay somewhere to the south, perhaps in the vicinity of the meandering Gulf Stream. Using the same dataset, Hogg (1981) applied ray tracing techniques to trace the origin of these waves back to a region where a trough in the Gulf Stream path was undergoing rapid evolution (as observed in satellite infrared imagery).

Bursts of topographic Rossby wave activity were also observed by Louis et al. (1982) on the continental slope south of Nova Scotia from an array of eight current meter moorings. Four intense wavelike events were identified over a one-year period. During these events, the deep velocity fluctuations over the slope were vertically coherent, usually barotropic, and had periods between 10 and 21 days. Bottom trapping was not observed. Coherence and phase estimates between various mooring sites indicated that phase was propagating offshore, suggestive of onshore energy propagation. In a companion paper, Louis and Smith (1982) developed a linear barotropic theory showing that such low-frequency oscillations on the slope could be produced by the shoreward excursion of a Gulf Stream meander or warm core ring. Farther offshore (near the HEBBLE site), Welsh et al. (1991) also observed wavelike motions with an approximately 30-day period that exhibited many of the properties of linear topographic Rossby waves. The motions were coherent over the array and indicated southwestward phase propagation and northwestward energy propagation. Observations inshore of the Gulf Stream near Cape Hatteras have also indicated onshore energy flux via topographic Rossby waves (Johns and Watts 1986). Schultz (1987) was even able to trace a burst of topographic wave activity near Cape Hatteras to a specific meandering event in the nearby Gulf Stream.

These observations have led to the development of a series of wave radiation models in which meander-like forcing applied at one boundary of a homogeneous fluid produces barotropic Rossby waves that radiate energy away from the boundary (Malanotte-Rizzoli et al. 1987; Hogg 1988; Malanotte-Rizzoli et al., in personal communication). From these model studies, it was determined that the forcing function must satisfy one critical condition in order for westward-propagating Rossby waves to be generated by eastward-propagating meanders: individual meanders must have a finite lifetime, with specific growth and decay stages. Only if the meanders have these transient characteristics can energy from the eastward-propagating meanders "leak" into adjacent frequency and wavenumber bands where westward propagation is possible. Observations of the Gulf Stream path based on satellite infrared imagery show that this condition is satisfied, suggesting barotropic wave radiation from the Gulf Stream should be possible.

To see if the radiation models could reproduce the observed distributions of eddy kinetic energy and Reynolds stress in the vicinity of the Gulf Stream, Hogg (1988) used a linear, stochastic wave radiation model to generate two-dimensional (x–y) maps of these quantities, and then compared the meridional structure of the maps to sections of EKE and Reynolds stress estimated from current meter records along 55°W. Agreement between the observational and model results was quite encouraging, especially considering the idealized nature of the model (linear, barotropic, uniform bottom slope). Both the model and the observations showed negative Reynolds stress north of the stream, and positive values to the south. This pattern is indicative of significantly polarized fluid motion in the NW–SE (NE–SW) direction north (south) of the forcing, consistent with northward (southward) energy radiation north (south) of the current. The *magnitudes* of Reynolds stress and EKE predicted by the model were also of the same order as those estimated from the data at 55°W.

The purpose of the present study is to characterize the observed EKE and Reynolds stress distributions for the entire Gulf Stream region and examine these distributions for evidence of radiating energy. Toward this end, we have combined all the available historical current meter data from the western North Atlantic and constructed maps of EKE and Reynolds stress in four frequency bands. The maps were then inspected for evidence of energy radiation away from the Gulf Stream, indicated for example by a pattern of negative Reynolds stress north of the stream and positive Reynolds stress to the south. Finally, we have qualitatively compared the large-scale features of the observed distributions to the maps of EKE and Reynolds stress generated from Hogg's linear model to assess the appropriateness of the model formulation.

Although many of the individual current meter records that make up the historical archive have been examined previously for evidence of radiated waves, this study is unique in at least two ways. First, we focus on evidence for radiated waves over a basinwide, O(1000 km), rather than local, O(100 km), scale. Second, we have averaged covariance estimates from all current meter records in a local area to improve the statistical significance of the estimates.

In the following section, the historical dataset and spectral and averaging techniques used in the analysis are described, and in section 3, we present the observed maps of EKE and Reynolds stress and discuss evidence for energy radiation from the Gulf Stream. Interpretation of the results and comparison with the model follows in section 4.

2. Data sources and statistical methods

Since the first long-term current meter moorings were deployed in the early 1970s, a vast amount of velocity data has been collected in the western North Atlantic from some 20–25 separate experiments. In an effort to facilitate continued analysis and study of these

observations, all known data records have been collected into one archive. This collection contains 607 time series of east and north (u, v) velocity components at depths from the sea surface to the ocean bottom in the region 30°–42°N, 80°–40°W. Most of the records also contain temperature time series, while only some include pressure. All time series in the archive have undergone similar initial processing; a low-pass filter was applied and the series were subsampled once daily (Schmitz 1974).

Since the focus of this work is on the deep barotropic circulation, only a subset of the archive including records from 2000 m and deeper (well below the base of the main thermocline) has been used. The subset has been further restricted to records longer than 128 days in order to allow division of all the time series into 128-day pieces. Although more degrees of freedom could have been gained by including the records shorter than 128 days and dividing the long records into shorter pieces, the cost would have been the loss of estimates of energy levels and Reynolds stress at the low-frequency end of the mesoscale band (lowest resolvable frequency is equal to inverse piece length). Since this band contains a significant fraction of the total eddy energy (Schmitz and Luyten 1990), a compromise was made between maximizing the degrees of freedom and maintaining adequate coverage at the low-frequency end of the spectrum. In all, 191 records satisfy the depth and record length criteria. The positions of these moorings are shown in Fig. 1a. Note that there are less than 191 moorings shown; many moorings supported more than one instrument.

Horizontal maps of EKE and Reynolds stress were constructed for four frequency bands from the data records in the following manner, using a slight variation of the MATLAB spectral analysis program (Moler et al. 1987). Each record was divided into 128-day pieces, which were then prewhitened by first differencing to reduce the impact of the "redness" of the spectra before taking the Fourier transform. Auto- and cross-spectral densities were then calculated at 0.0078 cpd (128^{-1} d^{-1}) frequency intervals from the Fourier coefficients. The estimates were then averaged over the pieces, recolored, multiplied by 0.0078 to convert from energy density to energy, and finally grouped in four frequency bands to improve statistical confidence. The frequency bands are defined as follows: band 1—256 to 51 days (sum of first two estimates in the spectrum); band 2—51 to 20 days (sum of estimates 3–6); band 3—20 to 11 days (sum of estimates 7–11); and band 4—11 to 7.8 days (sum of estimates 12–16). These bands span the range from the mesoscale down to near the high-frequency cutoff for topographic waves on the continental slope off the U.S. east coast (Johns and Watts 1985).

After auto- and cross-spectral estimates were calculated for each record and summed in frequency bands, the estimates were further averaged spatially in 5° longitude by 2° latitude boxes. Figure 1b shows the configuration of the averaging bins and the total number of data days included in each bin. The objective here again was to maximize the statistical reliability of the estimates of EKE and Reynolds stress in each frequency band.

In this spatial averaging process, we have assumed that the statistics of the flow field are homogeneous within each box and that each record is independent. There are some boxes for which this is not very accurate, such as near the Gulf Stream or in regions where the bottom slope changes rapidly. However, we have found that subdividing the averaging boxes into smaller regions does not change the qualitative characteristics of the large-scale patterns.

3. Results

a. Mean velocities

Figure 2 shows the mean velocity and its standard error for each of the averaging bins. The tail of each vector has been placed at the center of the averaging bin, with the exception of the two vectors in the northwest corner of the domain, which have been placed close to the moorings just offshore of the 2000-m isobath (see Fig. 1a). The standard error boxes associated with each vector indicate the statistical significance of each estimate of the mean at the 90% confidence level. That is, vectors that extend outside the boxes represent estimates of the mean velocity, that are significantly different from zero at the 90% confidence level. The number of degrees of freedom for each estimate of the mean was obtained by dividing the number of data days by 10, an approximate value for the integral time scale.

Evidence for a deep mean eastward flow associated with the Gulf Stream is apparent at 70°, 60°, 55°, and 50°W. The absence of a deep stream at 65°W is probably a result of the location of the single mooring within the box (Fig. 1a). Westward flows are indicated both to the north and south of the deep Gulf Stream. Mean speeds to the north are generally larger than those to the south, with some estimates exceeding 5 cm s^{-1}. Nearly all the estimates north of the stream are significantly different from zero.

South of the stream, the mean flow is generally weaker (<5 cm s^{-1}) with three notable exceptions. The first is at 35°N, 55°W, where Owens and Hogg (1980) have shown that the deep westward flow is locally enhanced by a small bump in the sea floor. The second is near 35°N, 70°W, where a persistent southwestward flow was observed for over 400 days along a 100-km-wide slope between the 4500-m and 5400-m isobaths at the base of the continental rise. The third is on the side of the Blake–Bahama Spur. In all three cases, it appears that the flow has also been locally accelerated by convergence in the isobaths.

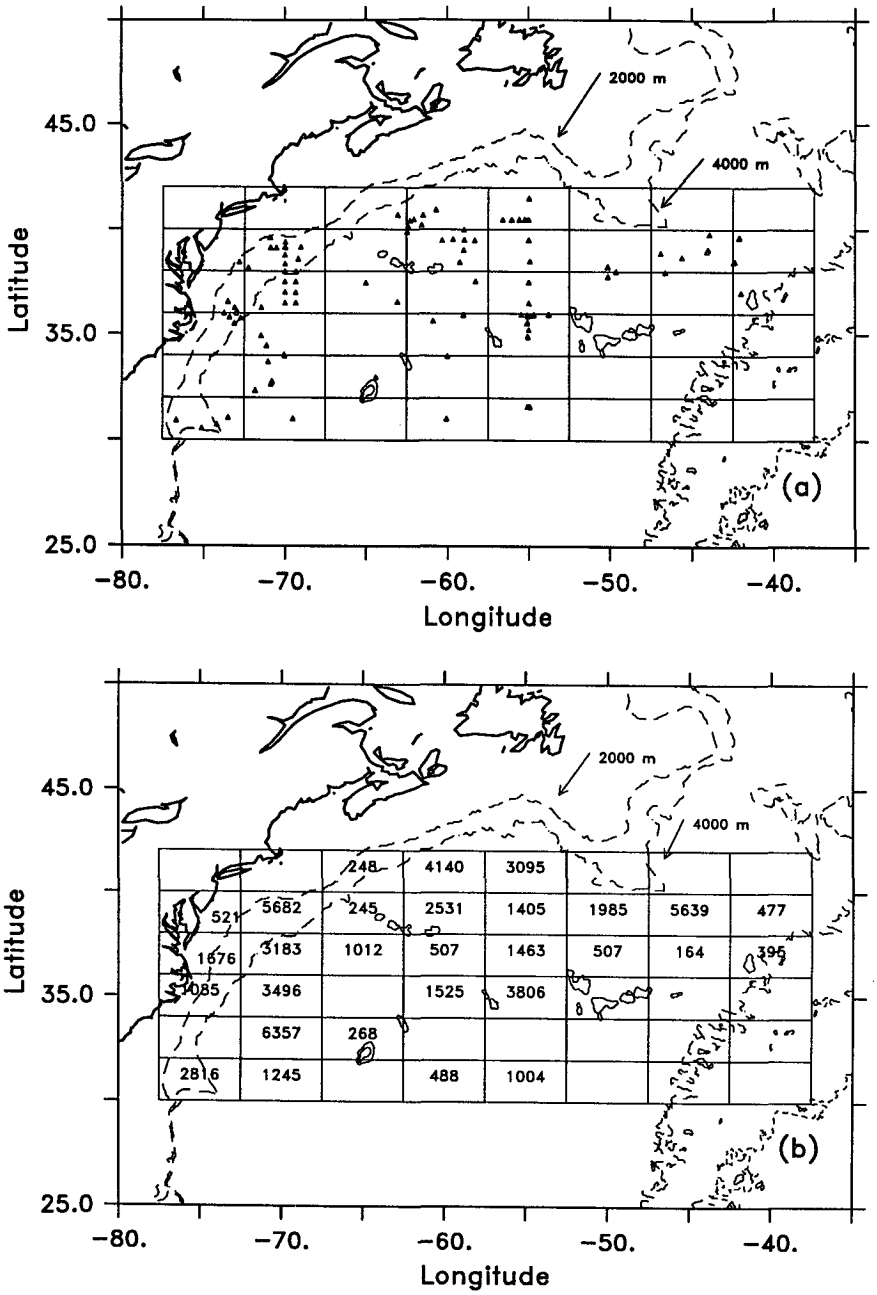

FIG. 1. (a) Locations of the moored current meter measurements used to examine the distributions of Reynolds stress and eddy kinetic energy. The rectangles define the spatial averaging scheme. The 2000-m and 4000-m isobaths are shown by dashed lines. (b) Total number of days of data in each averaging box.

b. Eddy kinetic energy maps

The maps of deep EKE constructed from the historical current meter data are shown in Fig. 3 for the four frequency bands defined in the last section. In each of these plots EKE per unit mass (in $cm^2\ s^{-2}$) is displayed. The heavy solid line running through the center of the domain shows the mean position of the Gulf Stream axis from Fig. 2. The 90% confidence limits for each estimate can be calculated using the graph in Fig. 4. The upper and lower limits are found by multiplying the energy estimate by the upper factor and lower factor for the appropriate number of degrees of freedom. For example, an averaging box with 1000 data days has seven complete 128-day pieces available and DOF = 56 if summing over two frequencies. The

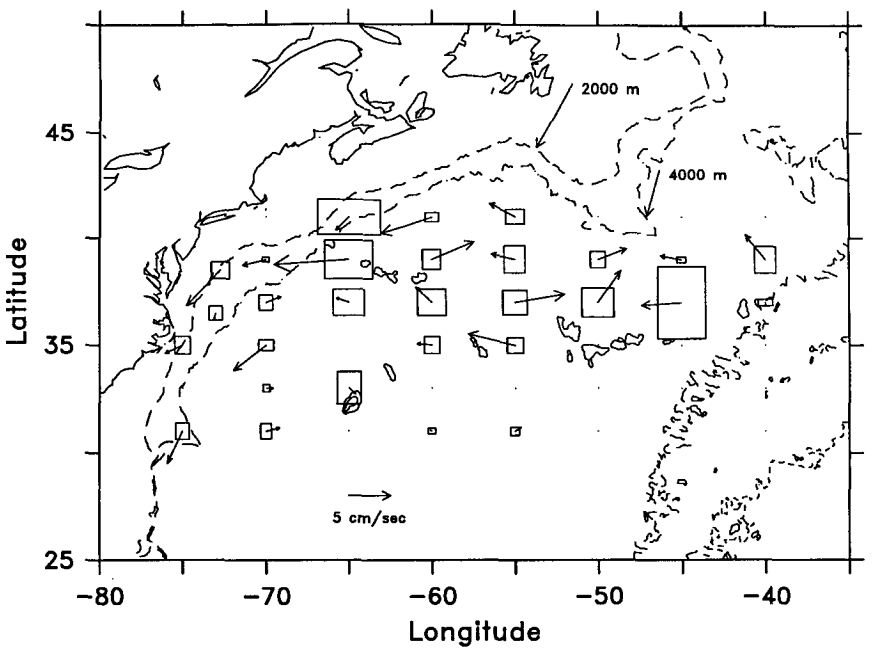

FIG. 2. Average velocity vectors for each box from all instruments at or deeper than 2000 m. The boxes indicate the standard error of the mean at the 90% confidence level.

upper factor would then be about 1.65 and the lower factor 0.67. For an energy level of 100 $cm^2\ s^{-2}$, the 90% confidence interval would be 165–67 $cm^2\ s^{-2}$.

In an idealized ocean, energy radiating from a meandering jet as linear barotropic Rossby waves should show up as areas of high eddy energy northwest and southwest of the maximum in meander activity (Hogg 1988). In the Gulf Stream, this meandering maximum is in the vicinity of 65°W where there is a maximum in surface eddy kinetic energy caused by large-amplitude energetic meanders (Richardson 1983). The distribution of deep EKE for the lowest frequency band, 256–51 days (Fig. 3a), representing the mesoscale band, shows a maximum along the mean axis of the Gulf Stream between 65° and 55°W. This figure resembles Schmitz's (1984) version of total EKE, most likely because the mesoscale band contains a large fraction of the total energy in the deep western North Atlantic (Schmitz and Luyten 1991). The maximum aligned with the stream axis reflects the energetic meandering of the Gulf Stream itself and makes it difficult to detect patterns that might indicate energy radiation to the northwest and southwest in the far field. There is some suggestion of southwest radiation in that energy levels south and west of 39°N, 65°W are all greater than 20 $cm^2\ s^{-2}$, while those south and east are significantly lower. North of the mean axis of the Gulf Stream, there is no strong evidence of northwestward radiation.

In the next three frequency bands, Figs. 3b–d, there is a distinct change in the large-scale pattern of EKE compared to the mesoscale band. Rather than being centered on the mean Gulf Stream axis, the maximum in deep EKE shifts north and west with increasing frequency. There is some evidence of southwestward energy radiation in the 51–20-day band (Fig. 3b), but none at higher frequencies. North of the Gulf Stream, the maximum shifts westward from 55°W in band 2 to 65°W in band 4, suggestive of NW radiation at higher frequencies. Note, however, that in the three highest frequency bands, the maxima are isolated on the continental rise and do not appear to be "connected" to the hypothesized source (the stream) by a ridge of high energy.

These EKE distributions taken by themselves must be considered inconclusive regarding evidence for energy radiation via Rossby waves. In a recent study of energy radiation from the Kuroshio Extension, Tai and White (1990) make the same point after analyzing the distribution of variability in sea surface height measured with the Geosat altimeter. In both cases, the velocity fluctuations produced by the meanders themselves seem to mask the radiating signal.

c. Reynolds stress maps

The distribution of Reynolds stress can be used more effectively to identify radiating Rossby waves in this region because the meandering of the jet does not generate any significant covariance between the velocity components. The magnitude of the Reynolds stress combined with the phase lag between the velocity components is a powerful indicator of the polarized motion characteristic of Rossby waves. Based on linear

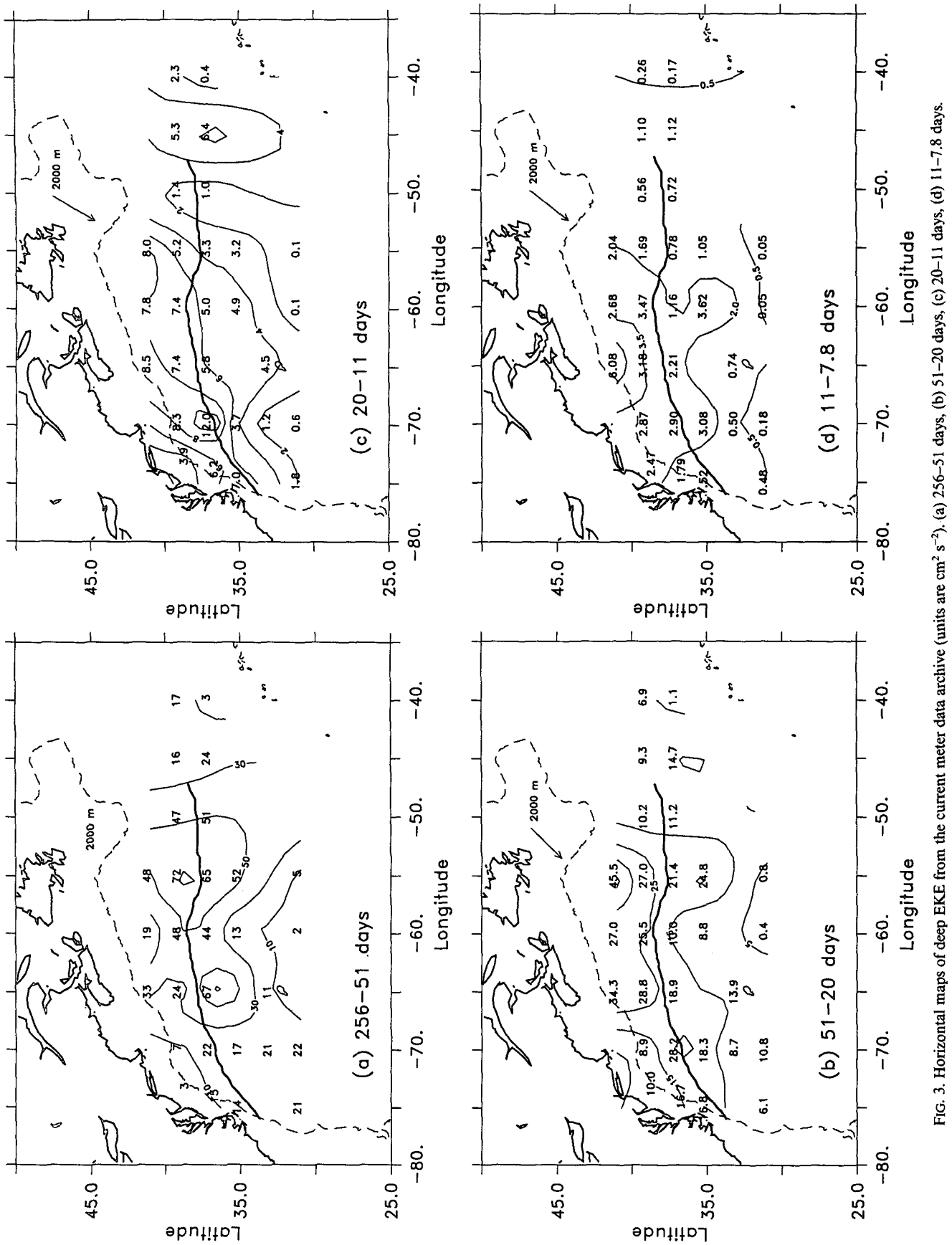

FIG. 3. Horizontal maps of deep EKE from the current meter data archive (units are $cm^2\ s^{-2}$), (a) 256–51 days, (b) 51–20 days, (c) 20–11 days, (d) 11–7.8 days.

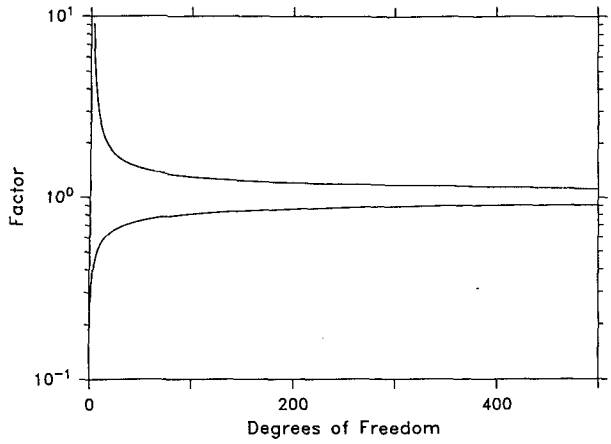

FIG. 4. Plot for determining 90% confidence limits on EKE estimates in Fig. 3. See text for explanation.

Rossby wave theory, northward energy radiation would imply southwestward phase propagation with fluid motions generally polarized in the northwest–southeast quadrants producing a negative covariance (velocity components 180° out of phase). Likewise, southward energy radiation implies northwestward phase propagation with motion polarized in the northeast–southwest quadrants (positive covariance; u and v in phase). Below we examine the distributions of Reynolds stress in the frequency domain (cospectrum and phase) for patterns indicative of outward radiation from the Gulf Stream.

In Fig. 5, the distribution of the average uv cospectrum and the uv phase for the mesoscale band is shown (positive phase means v leads u). Units are the same as for EKE. Enlarged numerals indicate statistically significant coherence amplitude between u and v at the 90% confidence level. Asterisks are used to mark those estimates that have the sign consistent with Rossby wave radiation. We restrict our attention to the area west of 50°W (inclusive) where the most energetic meandering takes place.

North of the Gulf Stream, where northward energy flux by Rossby waves would produce predominantly negative Reynolds stress, less than half of the estimates are less than zero, and there is no evidence of u and v being 180° out of phase. South of the stream, there are many positive values, which would suggest southward radiation, but only four estimates indicate that u and v are in phase within the 90% confidence intervals (indicated by asterisks).

Although the Reynolds stress estimates do not at first glance seem to indicate widespread outward energy radiation through Rossby waves, especially north of the stream, if we consider the propagation characteristics of topographic waves along variable topography, it is possible to understand why the expected signal may not be apparent. Rhines (1971) has shown that Rossby waves approaching a region of gradually changing bottom slope will be refracted as illustrated in Fig. 6. Rossby waves radiating northwestward from the Gulf Stream would propagate first across a relatively flat area, then across the gently sloping continental rise, and then onto the steeper continental slope. The shape of the basin north of the stream, which is somewhat semicircular, will lead to polarization of the fluid motion in the southwest–northeast direction there, shown by ray A. This motion will generate positive Reynolds stress and u and v will be in phase, as is the case for many of the estimates north of the stream in Fig. 5. While we might not expect such strong refraction south of the stream, where the bottom is relatively flat on large spatial scales, in fact, many moorings were deployed on locally steep topography where refraction or wave scattering could be taking place.

The effect of this refraction can be removed by rotating the coordinate system to one aligned with the local ambient potential vorticity gradient, including both the planetary and topographic effects. In this new coordinate system, "north" is directed up the ambient potential vorticity (PV_a) gradient, which is defined as

$$\nabla PV_a = -\left(\frac{f}{H}\frac{\partial H}{\partial x}\right)\mathbf{i} + \left(\beta - \frac{f}{H}\frac{\partial H}{\partial y}\right)\mathbf{j}. \qquad (1)$$

One can easily see that fluid motions associated with a wave packet traveling along ray A will produce a negative Reynolds stress when viewed in this new coordinate system (fluid motion polarized in the second and fourth quadrants of the new system). Rays propagating from the north, for instance, waves reflected from the shelf break (ray B), will also be refracted by the changing bottom slope. But since these rays see increasing, rather than decreasing, water depth, they will be refracted to the right when looking in the direction of energy propagation. In the coordinate system aligned with the local ∇PV_a, fluid motions associated with these rays will produce *positive* Reynolds stress. When viewed in the geographic system, both rays generate a positive Reynolds stress. Therefore, it is important to rotate the coordinate system to one aligned with the local ambient potential vorticity gradient in order to correctly identify the direction of energy propagation over sloping topography.

To recalculate the uv covariances in the new coordinate system, it was necessary to estimate the local bottom slope at each mooring site. This was done using a digitized database consisting of ocean depth measurements every 5 minutes of latitude and longitude for the world's oceans (National Geophysical Data Center). The true east and north components of the bottom slope were estimated by linear regression of the ocean depth measurements over 100 km in both directions, centered at the mooring site. The direction of upslope is then given by the arctangent of the north component of bottom slope divided by the east component. A horizontal scale of 100 km was chosen over

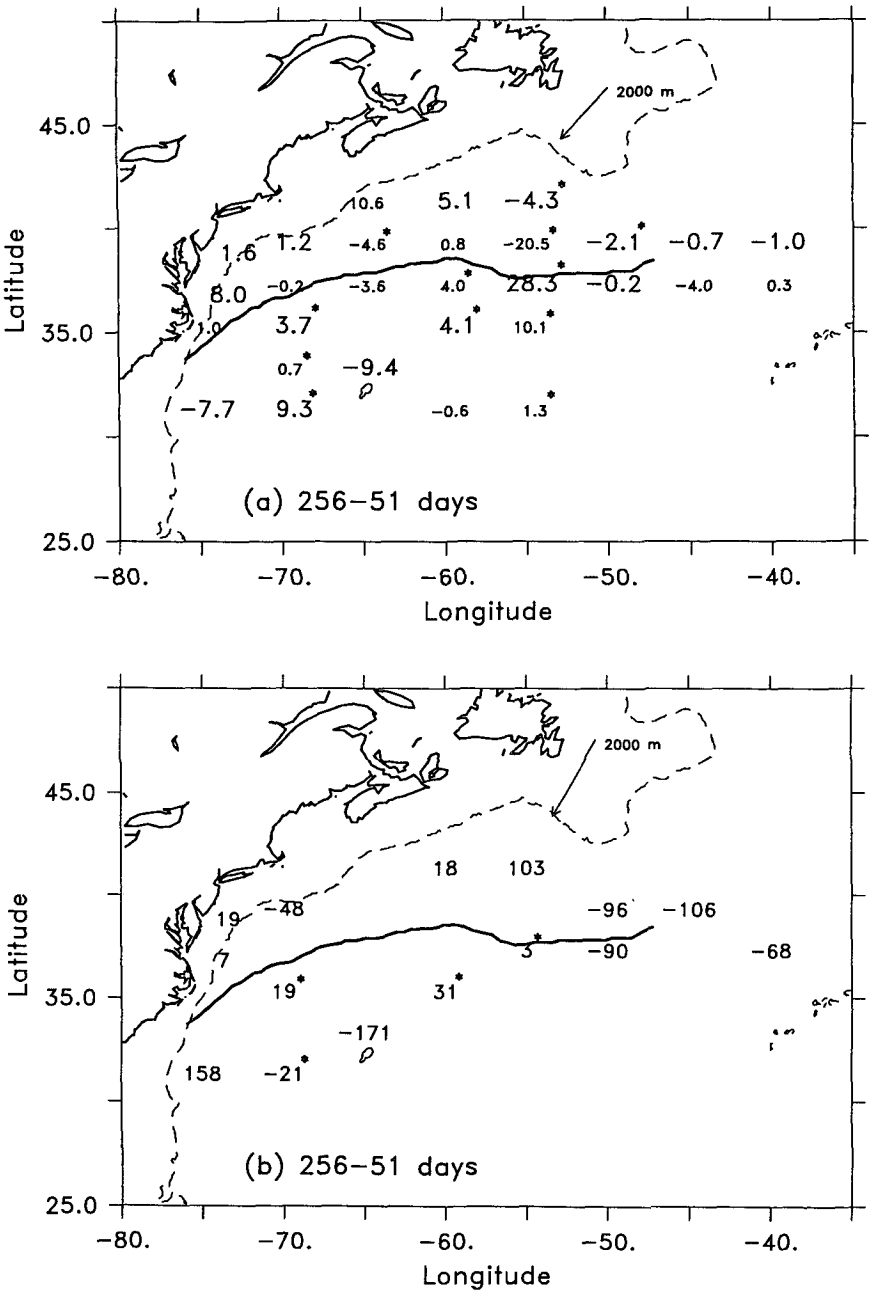

FIG. 5. Distribution of average (a) u, v cospectrum and (b) u, v phase for band 1, 256–51 days. In (a), enlarged numerals indicate statistically significant coherence amplitude. Asterisks indicate estimate is of the correct sign for wave radiation from the Gulf Stream, negative north of the stream, and positive south of the stream. In (b), positive phase means v leads u, and asterisks indicate phase lags are consistent with wave radiation within the 90% confidence limits, 180° north of the stream, and 0° to the south.

which to estimate the bottom slope. It is not completely clear over what spatial scale the Rossby waves may be affected by changing topography. Different wavelengths probably respond to different spatial scales. The 100-km scale was chosen to represent an average wavelength.

Figure 7a shows the direction of increasing ambient potential vorticity at each mooring. The length of each vector is proportional to the amplitude of the gradient. The vectors are displayed again in Fig. 7b without the 2000- and 4000-m isobaths so the arrows can be seen more clearly. North of the stream, where most of the

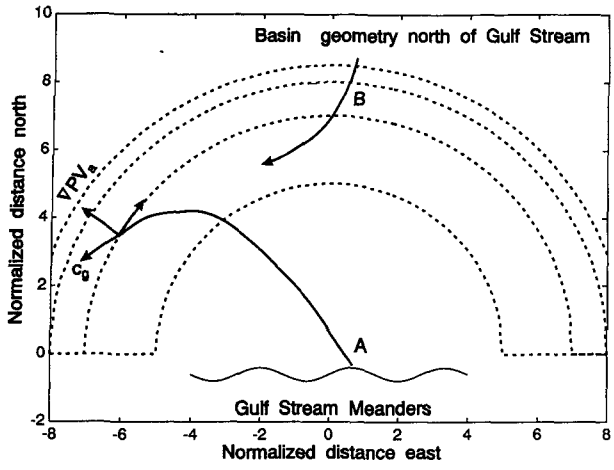

FIG. 6. Schematic diagram showing effect of bottom topography on Rossby wave refraction. North of the Gulf Stream, the northward increase in bottom slope may cause waves to be refracted as shown.

moorings were placed over the continental rise, the ambient vorticity gradient is controlled by the topography and the vectors point basically upslope. South of the stream, the bottom is generally flatter, particularly in the Sohm and Hatteras Abyssal plains, and the small vectors there represent the planetary vorticity gradient alone. There are a significant number of moorings, however, that were deployed on locally steep bathymetry. Examples are on the north side of the Bermuda Rise, on the Blake–Bahama Outer Ridge, and on an extension of the continental rise at 35°N, 70°W. The range in direction of the vectors around 35°N, 60° and 55°W gives an indication of the small-scale roughness of the bottom in this region. The sea floor north of the stream, although steeper, is considerably smoother. This roughness south of the stream will be considered later in relation to scattering of Rossby waves there.

Figure 8 shows the distribution of *uv* cospectrum and *uv* phase for each frequency band in the coordinate system aligned with the local ambient potential vorticity gradient. As in Fig. 5a, estimates marked with an asterisk are of the "correct" sign for wave radiation away from the Gulf Stream (negative to the north, positive to the south).

In the mesoscale band (Fig. 8a), all but one of the estimates north of the stream are negative, consistent with Rossby wave radiation from the Gulf Stream. Despite the lack of statistical significance, the abundance of negative values suggests a real signal is present. Because of the lack of statistical significance of most of the estimates, only a few phase estimates are available (Fig. 8b), and they do not show the phase relationship between u and v that would indicate radiating Rossby waves. South of the stream, the sign of the cospectrum is not as uniform as to the north; there are about as many positive as negative values. Only one of the estimates has the expected phase relationship.

In the next two frequency bands, the evidence for radiating Rossby waves is quite striking north of the Gulf Stream. Most of the cospectral estimates are less than zero, and many indicate that the velocity components are statistically correlated and nearly 180° out of phase. In both bands, the maximum covariance is found in the vicinity of 41°N, 65°W (this feature will be discussed further in the next section).

South of the stream, there are about as many negative as positive values, as was the case in the lower frequency band. Again, only a few of the phase estimates here show the appropriate phase relationship for wave radiation.

In the highest frequency band (Figs. 8g and 8h), there are nine estimates less than zero north of the stream, with the extreme again at 41°N, 65°W. Only two of these estimates, however, show u and v to be 180° out of phase within the 90% confidence intervals. South of the stream, the results are similar to those for the lower frequency bands.

To summarize the observed Reynolds stress maps, these distributions show negative Reynolds stress over large portions of the region north of the Gulf Stream in all frequency bands, strong support for the presence of radiating Rossby waves. The strongest evidence exists in the middle two bands where u and v appear to be statistically correlated and 180° out of phase. Evidence for wave radiation north of the stream is less strong in the highest and lowest frequency bands where u and v were found to be statistically incoherent at many locations and where the expected phase relationship was found only in isolated areas. South of the stream, there is little evidence of Rossby wave radiation.

d. Variance ellipses

Further evidence to support widespread topographic wave activity north of the Gulf Stream is apparent from the average variance ellipses shown in Fig. 9. The orientation of each ellipse is shown *relative* to the direction of the ambient potential vorticity gradient in the box; the ordinate of the superimposed axes points toward increasing ambient potential vorticity (upslope on continental rise) and the abscissa is directed along lines of constant PV_a [see Eq. (1)]. Calman (1978) presents a thorough discussion of the construction and interpretation of two-dimensional hodographs.

In the lowest frequency band (Fig. 9a), the ellipses are in general oriented nearly along the isobaths over the continental rise and slope from the Blake Escarpment south of Cape Hatteras, to the Grand Banks. The variance is not directed *exactly* along the lines of constant PV_a; the inclination into the second and fourth quadrants gives the negative cospectrum discussed earlier, which is indicative of energy radiation from the

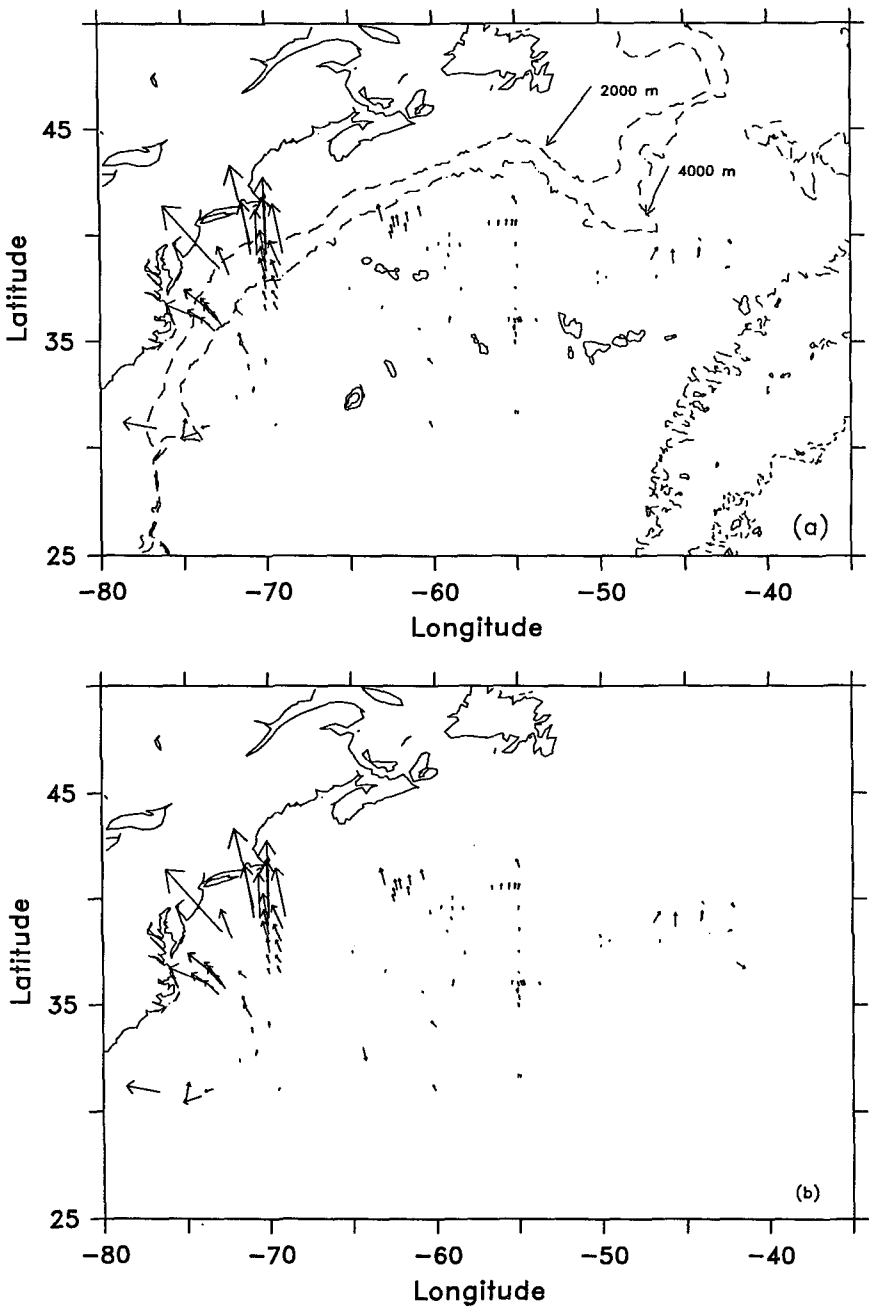

FIG. 7. (a) Magnitude and direction of β_{eff} (or ambient potential vorticity gradient) at each of the mooring sites. Small arrows in flat areas reflect planetary β only. (b) Same as (a) but without bathymetry contours.

south via Rossby waves. Some of the ellipses along the mean path of the Gulf Stream indicate a slightly greater degree of isotropy, perhaps due to meandering of the current over the moorings. Also of interest is the *lack* of isotropy over the Hatteras (31°N, 70°W) and Sohm (37°N, 55°W) Abyssal plains. With no strong topographic constraint, one might have expected less coherence between the velocity components. Of course, the planetary β effect does maintain some potential vorticity gradient in these areas.

As one moves to higher frequencies (Figs. 9b–d), there is a tendency for the major axes of the ellipses on the slope and rise to rotate toward an alignment *across*, rather than along, the isobaths. Good examples

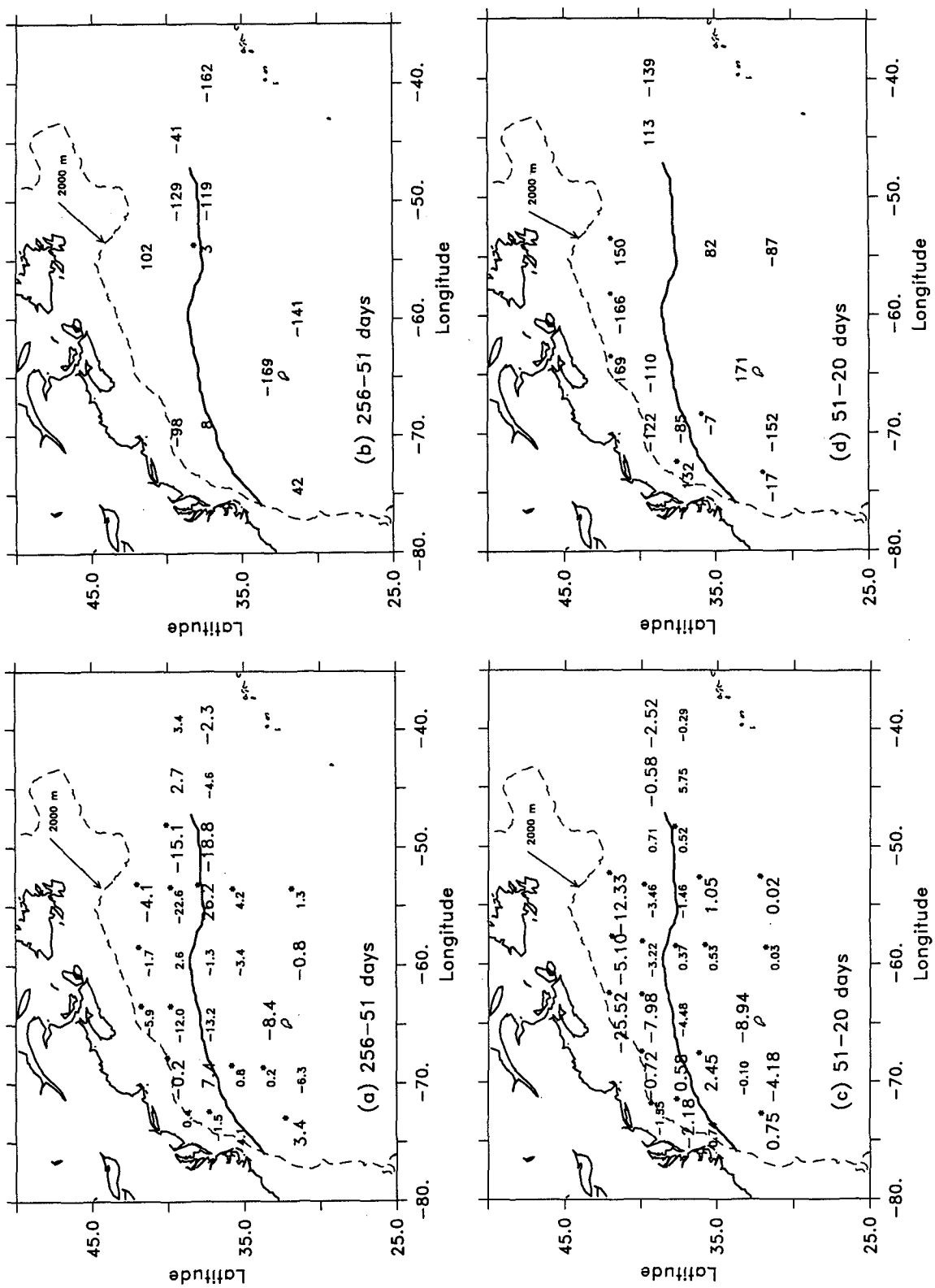

FIG. 8. Cospectrum and phase distributions for a coordinate system aligned with the ambient potential vorticity gradient. Annotations are the same as for Fig. 7. (a–b) 256–51 days, (c–d) 51–20 days, (e–f) 20–11 days, (g–h) 11–7.8 days.

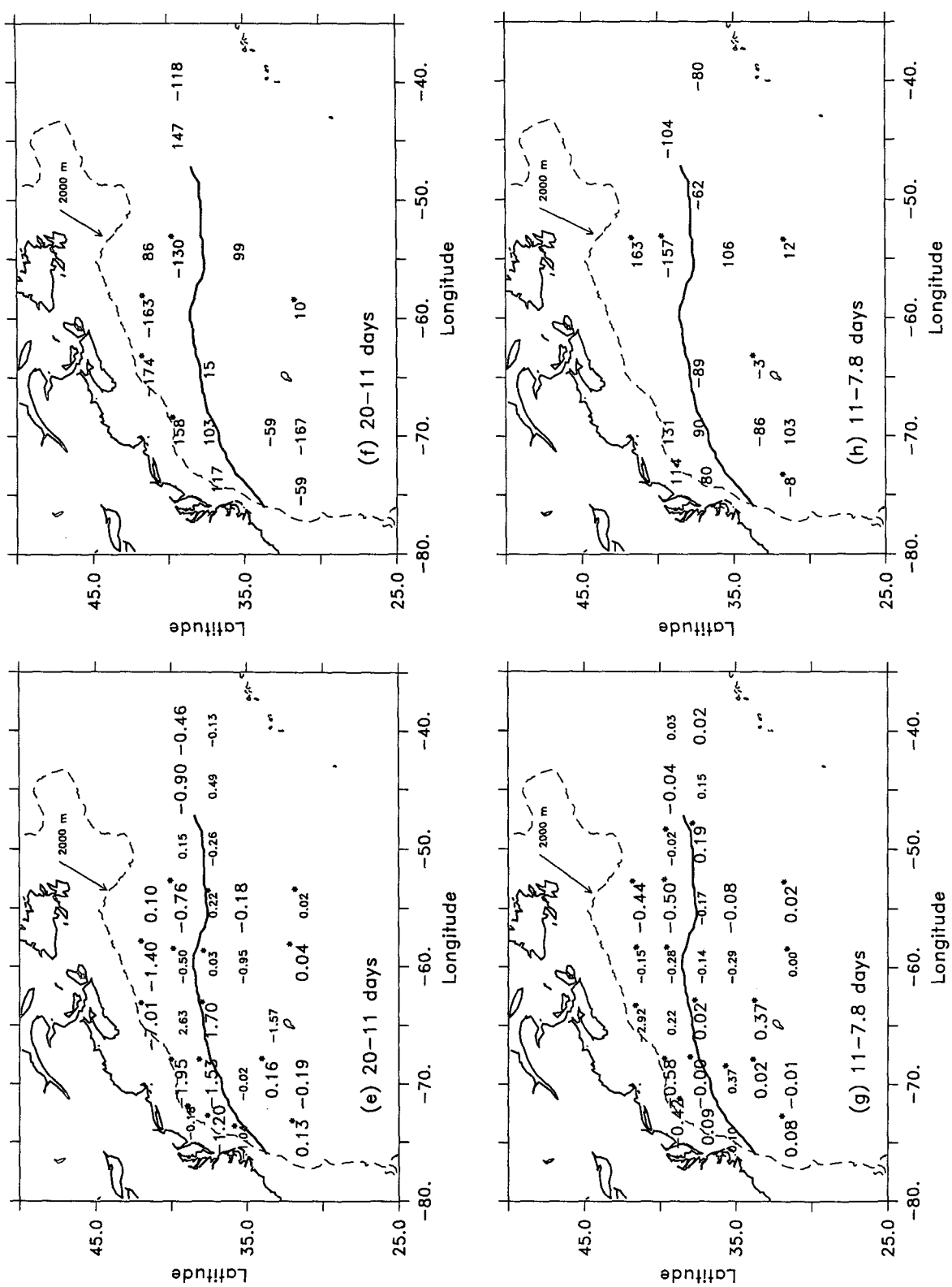

FIG. 8. *(Continued)*

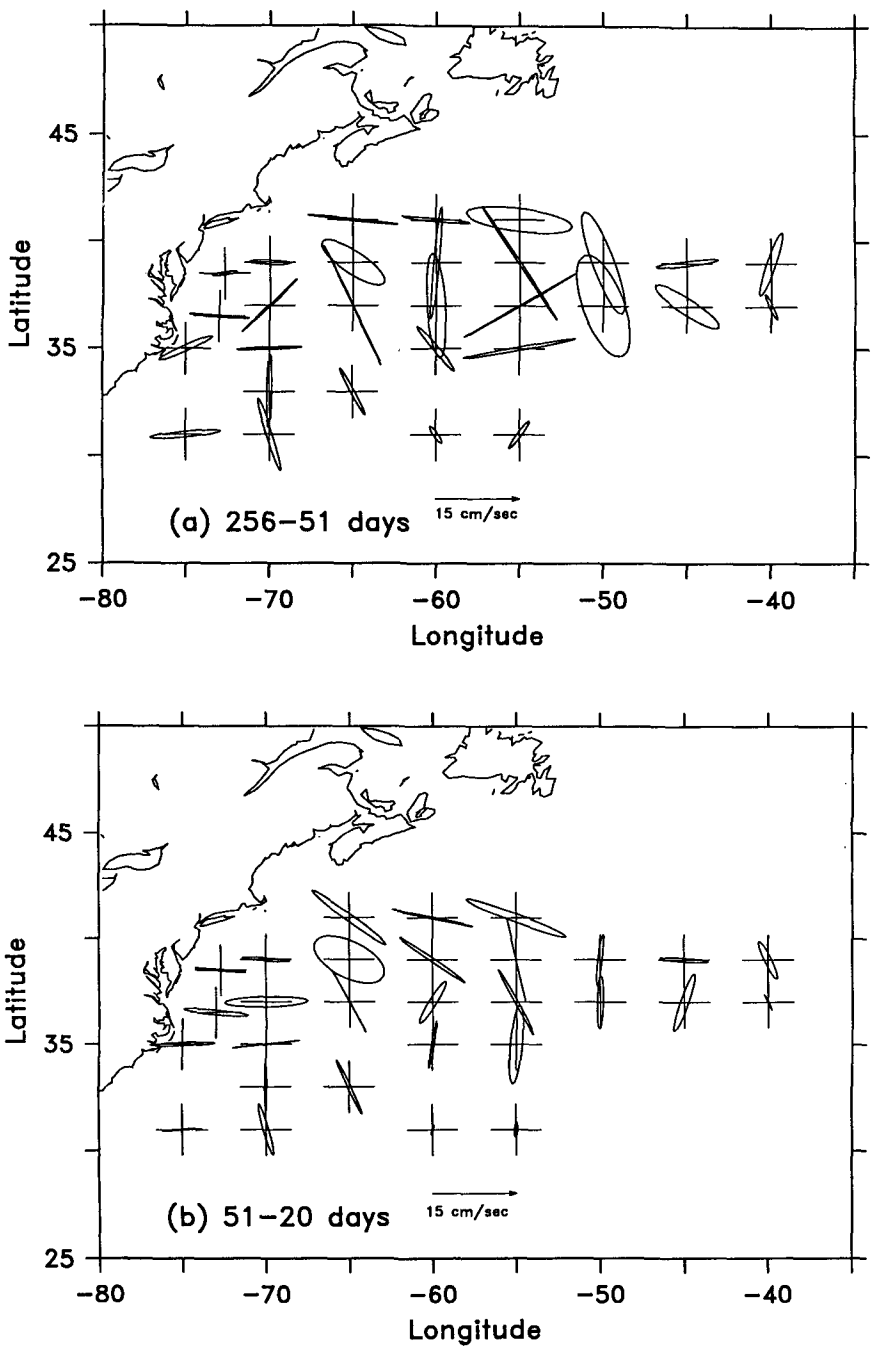

FIG. 9. Rotary variance ellipses for velocity components relative to local ambient potential vorticity gradient (indicated by small axes). Ordinate points in direction of increasing PV_a. (a) 256–51 days, (b) 51–20 days, (c) 20–11 days, (d) 11–7.8 days. Many ellipses on slope and rise rotate with increasing frequency indicative of topographic Rossby waves.

of this are at 41°N, 65°, 60°, and 55°W, and at 37°N, 70°W. This rotation of the major axis with increasing frequency is a characteristic of topographic Rossby waves. Thompson and Luyten (1976) give an expression for this rotation as a function of frequency and environmental parameters,

$$\omega = N\alpha \sin\theta,$$

where ω is the wave frequency, N is the Brunt–Väisälä frequency, α is the bottom slope, and θ is the angle to the right of an observer facing downslope of the wavenumber vector $\vec{\mathbf{k}}$. In the low (high) frequency limit, $\vec{\mathbf{k}}$

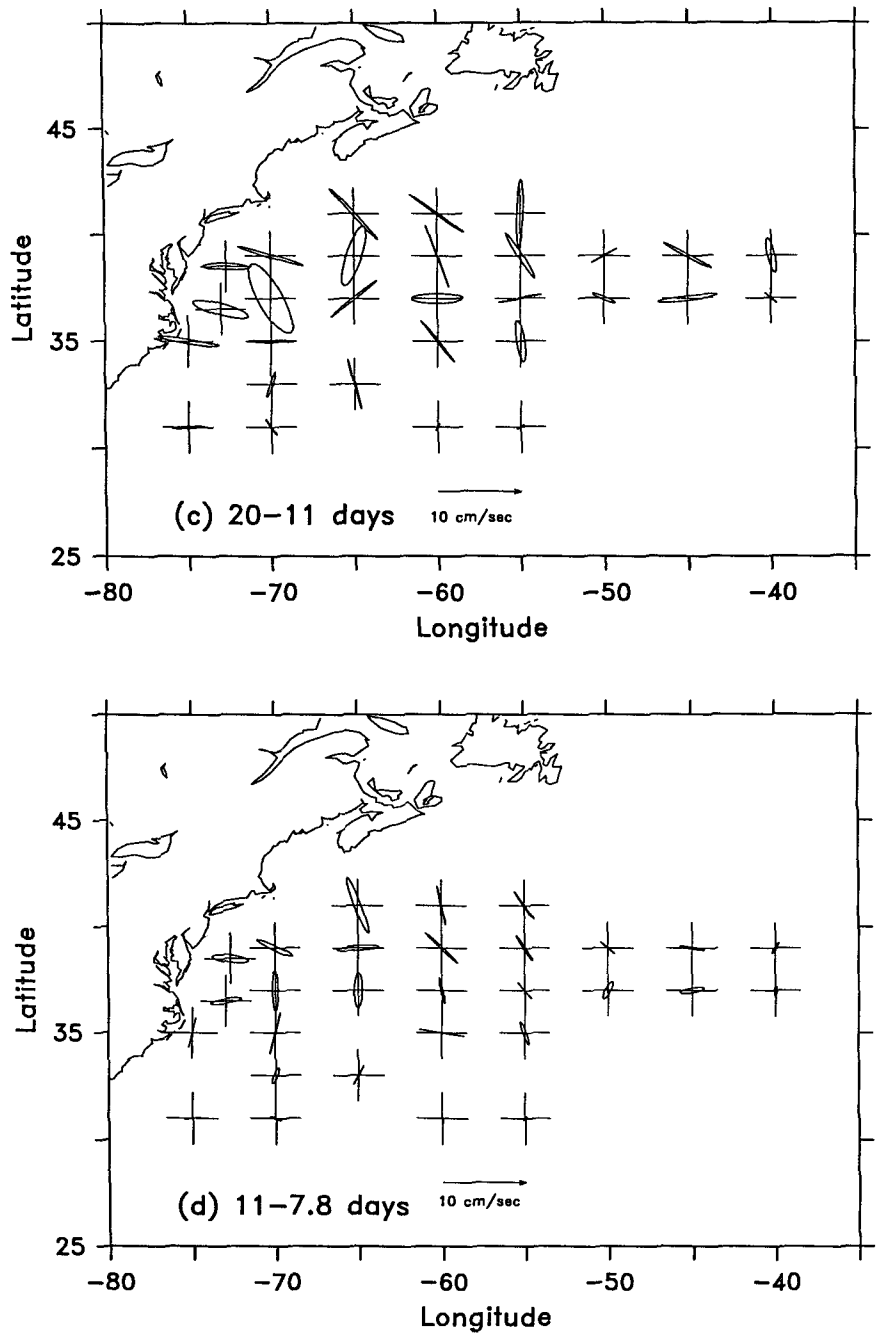

FIG. 9. (*Continued*)

is oriented down (along) the isobaths, and fluid particle motions are directed along (across) the isobaths. For typical values on the slope of $\alpha = 10^{-2}$, $N = 10^{-3}$, the highest frequency topographic Rossby waves have periods on the order of 7–8 days. The rotation of the variance ellipse with frequency has been observed in individual current meter records from the continental slope and rise and has been documented by several investigators (e.g., Johns and Watts 1986; Schultz 1987). The results presented here suggest that the wave activity is not localized, but distributed over a large portion of the area north of the Gulf Stream.

In the previous subsection, it was mentioned that in the highest and lowest frequency bands examined, *uv* coherence amplitudes were generally not significant, while in the middle bands, statistically significant coherence amplitude was observed. A possible explanation for this is related to the coordinate transformation

and the orientation of the variance ellipses. It is easily shown that when the principal axes of variance are aligned with the chosen coordinate system, the coherence amplitude reaches its minimum value (Fofonoff 1969). Thus, in the lowest frequency band, where the major axes of the variance ellipses tend to be nearly aligned with the isobaths (or isolines of ambient potential vorticity), the abscissa in our rotated coordinate system, a minimum in coherence is expected. Likewise, in the highest frequency band, where the major axes have a tendency to be oriented nearly perpendicular to the isobaths, along the ordinate, the coherence also approaches a minimum. In between these limits, where the wavenumber vector and ellipse orientation cross the isobaths at some oblique angle, coherence amplitude reaches its maximum value. This could explain the relatively high coherence levels observed in the middle two frequency bands, and the lack of coherence at the upper and lower ends of the spectrum. Radiating waves probably exist in the highest and lowest bands, but they are difficult to detect in the potential vorticity coordinate system.

4. Discussion

In order to place these observed distributions of EKE and Reynolds stress in some context, in this section we compare the distributions to maps produced with the stochastic wave radiation model developed by Hogg (1988). Hogg found that the model (described briefly below) reproduced the observed meridional structure of EKE and Reynolds stress along 55°W quite well. With the maps presented above, we are in a position to examine the model results more critically by comparing both the zonal and meridional structure of the model output to the observations. Since the model is highly idealized (barotropic, linear, and uses a uniform bottom slope), our comparison can be only qualitative. More quantitative comparisons must await more sophisticated models (Malanotte-Rizzoli et al., in preparation).

In the wave radiation model developed by Hogg, a homogeneous fluid layer is forced by a series of idealized, small-amplitude meanders that travel along a zonal boundary. The model is designed to simulate the Gulf Stream in the region downstream of Cape Hatteras, where meanders in the current's path grow and propagate downstream. Although the eastward-traveling meanders are mismatched to westward-propagating Rossby waves, transient features of the meanders (i.e., their growth and decay) leak energy into the radiation portion of the frequency–wavenumber domain. The details of the meander forcing function are not repeated here; interested readers are advised to consult Hogg (1988) for more information.

The model-generated maps of total EKE and Reynolds stress are shown in Fig. 10 for the region north of the forcing. (The general patterns of EKE and Reynolds stress are not strongly frequency dependent.) Here the planetary vorticity gradient, β, has been enhanced (doubled) by a bottom boundary that slopes up uniformly to the north to simulate the continental rise north of the Gulf Stream. South of the forcing, the distributions are qualitatively similar (symmetric about the x axis), the primary difference being a change in sign of the Reynolds stress. The dashed curve indicates the downstream variation in the strength of the meander activity. The point of maximum width ($x = 0$ km) corresponds to about 65°W in the Gulf Stream system, where the maximum in surface EKE has been observed with drifter trajectories (Richardson 1983).

The highest energy levels (Fig. 10b and 10c) are found very close to the moving boundary and result from trapped eastward-propagating modes, which do not radiate energy outward. Away from the boundary, the zonal component of EKE is substantially greater than the meridional. This is due to the fact that the spectrum of the forcing function is peaked at low frequencies and low wavenumbers, generating Rossby waves with near zonally aligned crests and more energetic east–west motions (Hogg 1988). Although Rossby waves radiate energy away from the boundary in all directions (direction depends on frequency of individual waves), the average response shows energy radiating away from the maximum in the forcing toward the northwest (southwest) north (south) of the moving boundary.

The Reynolds stress structure in the model (Fig. 10a) also shows extreme values extending away from the maximum in the forcing toward the northwest (and toward the southwest south of the forcing, not shown). Only the radiating modes contribute to the Reynolds stress because, in the trapped modes, u and v are 90° out of phase.

a. Comparison of eddy kinetic energy

The two most striking features of the eddy kinetic energy distributions produced from the model are 1) the strong maximum near the forcing associated with the trapped modes, and 2) the lobes of high eddy kinetic energy northwest and southwest of the maximum forcing. In the observations, there is a distinct maximum over the mean stream position at low frequencies (Fig. 3a), but this feature is noticeably absent at higher frequencies (Figs. 3b–d) where the maximum shifts to the northernmost grid points. The stochastic forcing model contains trapped disturbances at all frequencies forced by eastward-propagating, time-dependent meanders; steadily propagating, unchanging meanders are incapable of coupling to Rossby waves. This use of eastward-propagating, time-dependent meanders in the model biases the wavenumber–frequency spectrum of the forcing to eastward propagation and enhances the energy in the trapped modes at all frequencies. It is, of course, possible that the trapped modes *are* present in

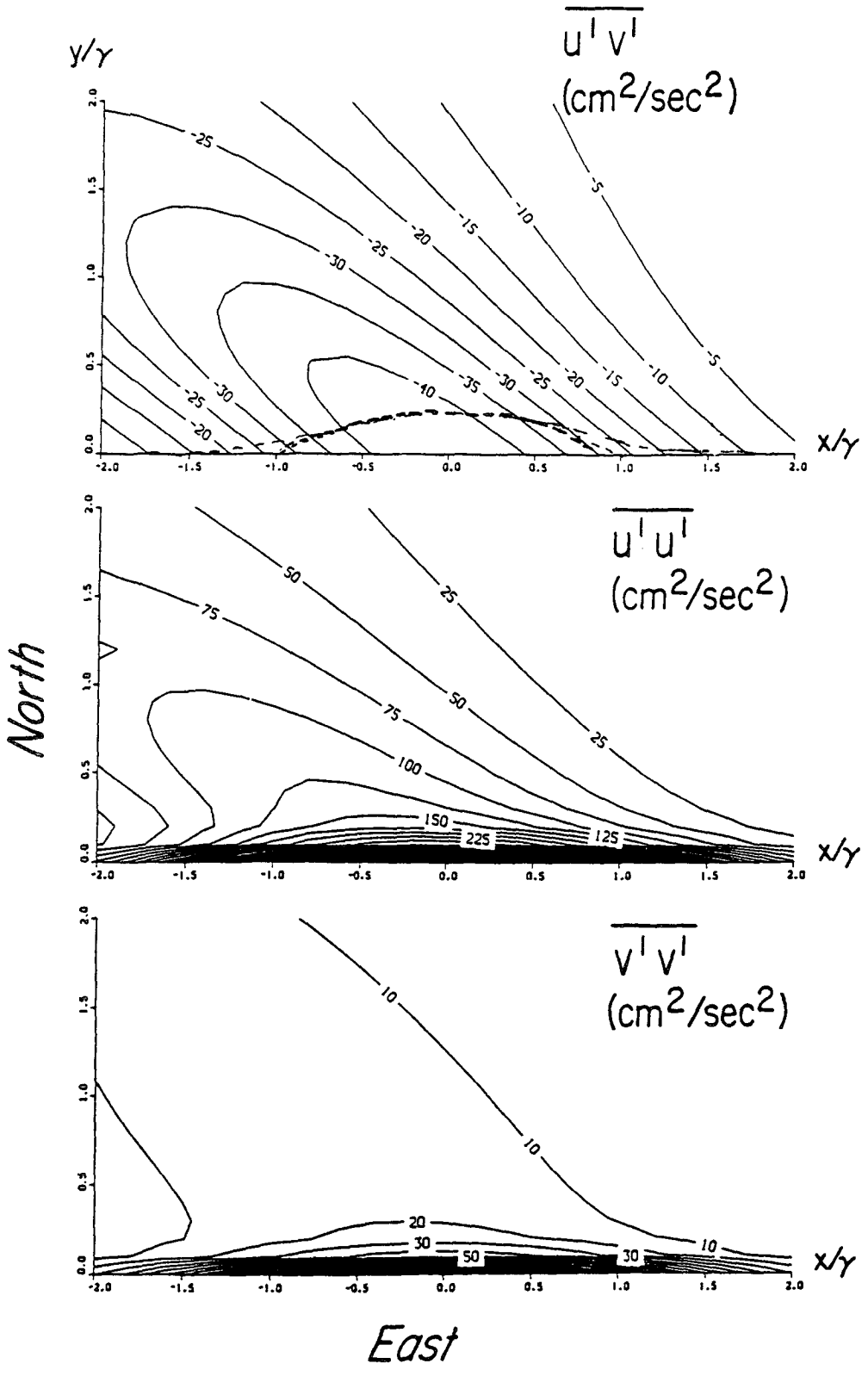

FIG. 10. Distribution of (a) Reynolds stress, (b) zonal component of eddy kinetic energy, and (c) meridional component of kinetic energy from Hogg's (1988) stochastic wave radiation model. Distance units have been nondimensionalized by 600 km. Only the region north of the forcing, where β has been enhanced by a uniform bottom slope, is shown.

the ocean but simply overwhelmed by other processes. However, the current meter results indicate that at the higher frequencies, there is no maximum associated with the stream and that eddy energy actually increases toward the north. It seems more likely, if the Gulf Stream is to be considered an energy source, that the simple meander forcing function used in the model is inadequate.

Some hint of this can be seen in the frequency–wavenumber spectra of the Gulf Stream front produced by Halliwell and Mooers (1983) from four years of satellite infrared observations. They see a dominance of eastward propagation at periods longer than about 30 days but more equipartition between eastward and westward propagation at higher frequencies. For periods shorter than about 20 days there is even a dominance of westward energy. It is unknown whether this westward propagation observed by Halliwell and Mooers results from meander time dependence, some other process, or even whether it is real. The topographic wave study of Louis and Smith (1982) is an example of a *stationary* Gulf Stream disturbance generating topographic waves.

There are other features of the real ocean circulation in this area not included in the model that may strongly influence the observed distributions. For instance, the *westward* shift in maximum EKE with increasing frequency may be due to zonal changes in meander characteristics. Meanders have typical wavelengths of around 250 km near Cape Hatteras increasing to 350 km near 55°W. They progress toward the east with an average phase speed that decreases from about 8 cm s^{-1} to 4 cm s^{-1} over the same distance (Gilman 1988). This implies dominant periods that increase from 30 days to 90 days moving west to east and that the eddy kinetic energy peak should shift westward with increasing frequency, as is observed (Fig. 3). In addition, the *total* EKE increases toward the east, reaching a maximum on the order of 100 cm^2 s^{-2} at 55°W. This could be produced by the deep Gulf Stream with peak instantaneous speeds of order 10 cm s^{-1} meandering over the mooring sites. The deep expression of the stream does intensify from west to east with the addition of the flow associated with the northern recirculation gyre east of the Seamount Chain near 65°W (Hogg et al. 1986). It seems possible that much of the eddy kinetic energy in this region is simply a result of the meandering activity of the stream.

The enhancement of wave energy toward the north and the associated north–south asymmetry across the stream axis can be explained using simple linear wave theory. We show in Fig. 11 ray trajectories emanating from a source offshore of an inclined slope meant to model the slope and rise south of Nova Scotia. These rays are calculated using linear topographic wave dynamics with the planetary beta term and uniform stratification. We assume that a WKB analysis is adequate although the starting wavelength is sufficiently large to make this dubious. As the waves progress up onto the slope they refract and shorten so as to become more consistent with the WKB approximation. We show two different periods (36 days and 10 days) with the same initial zonal wavelength (6280 km, total wavelength is 1400 km at 10 days and 800 km at 36 days). Such a long wavelength is needed at high frequencies as the waves are initially almost barotropic Rossby waves: the minimum possible wavelength is about 2200 km at 10-day periods.

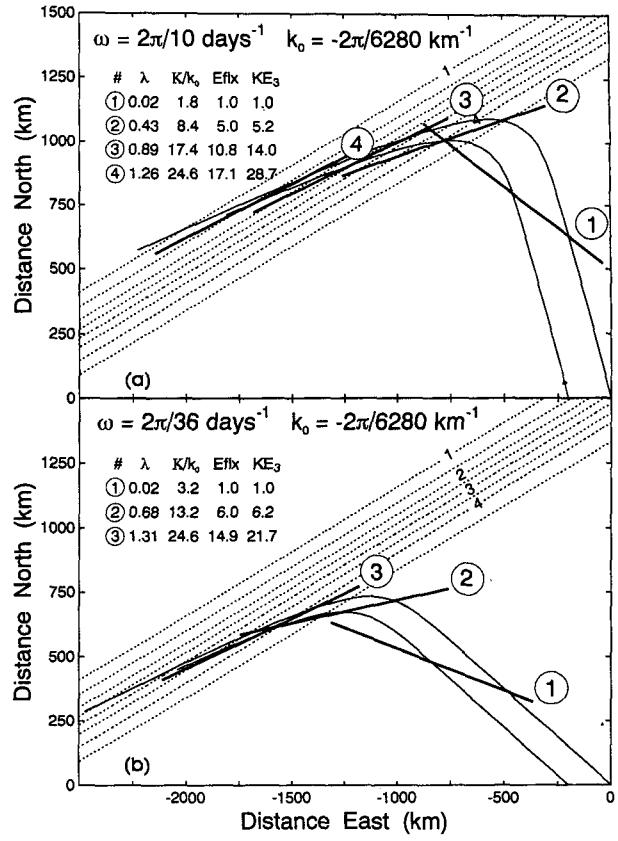

FIG. 11. Rays show pathway of energy propagation for barotropic–topographic Rossby waves approaching a steep slope. (a) wave period = 36 days, (b) wave period = 10 days. Tabulated values give the bottom intensification parameter with zero being barotropic and 1 moderate intensification, the wavenumber normalized by the initial zonal component, the energy flux normalized by the initial value, and the kinetic energy at 3000-m depth also normalized by its initial value at each of the wave crests.

For each period two neighboring rays are traced so as to show their convergence. Energy flow is along the ray and convergence is one factor in the change of energy density. Also shown are wave crests and along with the refraction of the ray comes a closer alignment of the wave crest with bottom topography. The higher frequency ray is less refracted and penetrates farther up the slope. The tabulated values give the bottom in-

tensification parameter, with zero being barotropic and 1 moderate intensification, the wavenumber normalized by the initial zonal component, the energy flux normalized by the initial value, and the kinetic energy at 3000-m depth also normalized by its initial value at each of the wave crests.

In this stratified example energy increases for three reasons. First, the rays converge as they are refracted and energy increases in inverse proportion to the ray separation. Second, refraction causes the wavelength to decrease; as group speed is proportional to wavelength squared (for barotropic waves, at least), this causes further buildup of the energy density. Finally, the stratification begins to play a role as the waves shorten and become bottom intensified. This leads to an increase in the kinetic energy of the deep water. All of these factors depend on the existence of the continental slope and will not play any significant role south of the stream. It is not difficult to have waves with enormous initial zonal wavelengths of order thousands of kilometers to become the short bottom-trapped waves observed on the rise and slope.

The sloping bottom associated with the continental margin may enhance low-frequency energy and covariance levels north of the stream in yet another way. Louis and Smith (1982) have shown theoretically that the formation and shoreward excursion of Gulf Stream meanders and rings up the continental rise can generate intense bursts of topographic waves with temporal and spatial scales similar to those observed (10–25 days; 50–200 km). As they point out, this strong radiation is possible because the characteristic phase speed of low-frequency oscillations, given by

$$c_{ph} \approx \beta L^2 \approx \frac{fL^2}{H}\frac{\partial H}{\partial y},$$

becomes much larger than U, the particle speed, as the waves move up the slope. Using values typical for the continental rise of $f \approx 10^{-4}\ \mathrm{s}^{-1}$, $L \approx 50$ km, $H \approx 3000$ m, and $\partial H/\partial y \approx .02$, $c_{ph} \approx 0.83\ \mathrm{m\ s}^{-1}$, which is an order of magnitude larger than typical particle speeds in the region. Thus, the slope tends to "linearize" the eddies and enhance barotropic radiation. South of the stream, there is no large-scale bottom slope; barotropic radiation from meanders and eddies therefore cannot be enhanced in the same way.

b. *Comparison of Reynolds stress*

The Reynolds stress distributions north of the stream provide the most convincing evidence for the presence of radiating Rossby waves when viewed in a coordinate system aligned with the local ambient potential-vorticity gradient. Negative values of the uv cospectrum are observed over a large area north of the stream in all frequency bands, consistent with northward energy radiation via Rossby waves. In addition, in the middle two bands, u and v appear to be statistically coherent and 180° out of phase at many locations, providing further support for the presence of radiating waves in these two bands.

The model appears to reproduce only the most basic feature of the observed Reynolds stress distribution; that is, the negative values north of the forcing (compare Figs. 10a and 8). The lobes of high Reynolds stress extending northwest and southwest from the forcing are not a prominent feature in the observations; there is only a hint of it in that the maximum value north of the stream in the highest three bands is found at 41°N, 65°W. Note that this estimate is isolated from the stream, unlike the model distribution, where there is a ridge of maximum covariance extending out from the maximum in the forcing. This patch of high covariance may again be the result of Rossby waves refracting and converging, or ring–meander interactions with the bottom slope as described above.

South of the stream, the covariance does not seem to have any recognizable pattern. As mentioned previously, this area is characterized by many small-scale bumps in the sea floor, which may lead to wave scattering. This would destroy any coherent pattern that might otherwise exist. In this respect, Hogg (1988) chose the most favorable area to make a model–data comparison of covariances (along 55°W where the ocean floor is relatively smooth). In addition, it has been shown by Hogg (1985) and Bryden (1982) that the Worthington recirculation gyre south of the Gulf Stream is baroclinically unstable. Disturbances generated as a result of this instability could easily mask the radiating signal.

In contrast to our observations, Tai and White (1990) found a much more consistent pattern of positive Reynolds stress south of the Kuroshio Extension between 145° and 170°E from altimetric observations. In fact, they see generally larger absolute values of the covariance south of the Kuroshio compared to north of the current. But as was the case in the Gulf Stream region, there is no strong evidence of the northwestward and southwestward extension of high covariance away from the maximum forcing that was seen in the model. A detailed comparative study of the two dynamically similar, but geographically different, regions could provide some insight into the effects of basin geometry, bottom topography, and forcing function (meander characteristics) on energy and Reynolds stress distributions.

Based on this discussion, therefore, it appears that the most important features that should be included in any future models of wave radiation from the Gulf Stream are a forcing function with more realistic wavenumber and frequency characteristics, and more realistic bathymetry and basin geometry. Work is cur-

rently underway to develop a numerical model that includes these features as well as finite-amplitude meanders.

5. Summary

We have used a compilation of all available current meter data from the western North Atlantic to look for evidence of Rossby waves radiating energy from the Gulf Stream. Auto- and cross-spectral estimates were calculated for each record and then averaged in 2° latitude by 5° longitude boxes to maximize the statistical reliability of the estimates. Horizontal maps of eddy kinetic energy and Reynolds stress were constructed to study the distributions of these quantities over as large a geographical area as possible. The maps were compared to similar distributions generated from a stochastic, barotropic wave radiation model.

The EKE maps, while exhibiting many interesting features, bear little resemblance to the model maps. We argue that this should be taken not so much as evidence against the presence of radiating disturbances, but more as an indication of the inadequacy of the model to reproduce the details of the EKE distribution. In particular, it was shown that the basin geometry and bottom topography, as well as the meander forcing function, which were greatly simplified in the model (to make the problem tractable), strongly influence the distribution of radiating energy.

When the uv cospectrum estimates were rotated into a coordinate system aligned with the local ambient potential vorticity gradient, the distributions north of the stream are consistent with northward energy radiation via Rossby waves. The evidence was particularly strong in the 51–11-day band, where 1) negative Reynolds stress was observed over a large geographical area, 2) u and v were on average 180° out of phase at many locations, and 3) the extremum was located northwest of the maximum forcing. In the highest and lowest frequency bands, it is harder to argue strongly for the presence of radiating waves due to the lack of statistically significant coherence between u and v, but this is probably due to the alignment of the principle axes of variance with the axes of the chosen coordinate system.

South of the stream, there was very little evidence of radiating Rossby waves. Since we expect that energy radiates away from the Gulf Stream equally to the north and south, and since there is strong evidence of wave radiation to the north, we suspect that energy does radiate outward to the south as well. However, the associated velocity fluctuations may be difficult to detect due to the scattering of Rossby waves by small-scale bathymetric features, and/or due to the overwhelming presence of other eddy generating processes such as baroclinic instability.

Acknowledgments. This work was supported by the National Science Foundation and the Office of Naval Research under Grant OCE86-08258 and Contract N00014-85-C-0001, NR 083-004. Part of this work was completed while A. Bower was a postdoctoral scholar at the Woods Hole Oceanographic Institution. We are grateful to Ann Spencer for assembling the current meter data archive. Comments by reviewers were extremely valuable in improving the manuscript.

REFERENCES

Bryden, H. L., 1982: Sources of eddy energy in the Gulf Stream recirculation. *J. Mar. Res.*, **40**, 1047–1068.

Calman, J., 1978: On the interpretation of ocean current spectra. Part I: The kinematics of three-dimensional vector time series. *J. Phys. Oceanogr.*, **8**, 627–643.

Cornillon, Peter, 1986: The effect of the New England Seamounts on Gulf Stream meandering as observed from satellite IR imagery. *J. Phys. Oceanogr.*, **16**, 386–389.

Fofonoff, N. P., 1969: Spectral characteristics of internal waves in the ocean. *Deep-Sea Res.*, **16**(Suppl), 59–71.

Gill, A. E., J. S. A. Green, and A. J. Simmons, 1974: Energy partition in the large-scale ocean circulation and the production of mid-ocean eddies. *Deep-Sea Res.*, **21**, 499–528.

Gilman, Craig S., 1988: A study of the Gulf Stream downstream of Cape Hatteras: 1975–1986. Master's thesis, Graduate School of Oceanography, University of Rhode Island, 77 pp.

Halliwell, G., and C. Mooers, 1983: Meanders of the Gulf Stream downstream of Cape Hatteras: 1975–1978. *J. Phys. Oceanogr.*, **13**, 1275–1292.

Hogg, N. G., 1981: Topographic waves along 70°W on the continental rise. *J. Mar. Res.*, **39**, 627–649.

——, 1985: Evidence for baroclinic instability in the Gulf Stream recirculation. *Progress in Oceanography*, Vol. 14, Pergamon, 209–229.

——, 1988: Stochastic wave radiation by the Gulf Stream. *J. Phys. Oceanogr.*, **18**, 1687–1701.

——, R. S. Pickart, R. M. Hendry, and W. J. Smethie, Jr., 1986: The northern recirculation gyre of the Gulf Stream. *Deep-Sea Res.*, **33**, 1139–1165.

Johns, W. E., and D. R. Watts, 1985: Gulf Stream meanders: Observations of the deep currents. *J. Geophys. Res.*, **90**, 4819–4832.

——, and ——, 1986: Time scales and structure of topographic Rossby waves and meanders in the deep Gulf Stream. *J. Mar. Res.*, **44**, 267–290.

Louis, J. P., and P. C. Smith, 1982: The development of the barotropic radiation field of an eddy over a slope. *J. Phys. Oceanogr.*, **12**, 56–73.

——, B. D. Petrie, and P. C. Smith, 1982: Observations of topographic Rossby waves on the continental margin off Nova Scotia. *J. Phys. Oceanogr.*, **12**, 47–55.

Malanotte-Rizzoli, P., D. B. Haidvogel, and R. E. Young, 1987: Numerical simulations of transient boundary-forced radiation. Part 1: The linear regime. *J. Phys. Oceanogr.*, **17**, 1439–1457.

Moler, C., J. Little, and S. Bangert, 1987: PRO-MATLAB for Sun Workstations. The Mathworks, Inc., Sherborn, MA, 01770.

Owens, W. B., and N. G. Hogg, 1980: Oceanic observations of stratified Taylor columns near a bump. *Deep-Sea Res.*, **27**, 1029–1045.

Pedlosky, J., 1979: *Geophysical Fluid Dynamics.* Springer-Verlag, 624 pp.

Rhines, P., 1971: A note on long-period motions at Site D. *Deep-Sea Res.*, **18,** 21–26.

Richardson, P. L., 1983: Eddy kinetic energy in the North Atlantic from surface drifters. *J. Geophys. Res.*, **88,** 4355–4367.

Schmitz, W. J., Jr., 1974: Observations of low-frequency current fluctuations on the continental slope and rise near Site D. *J. Mar. Res.*, **32,** 233–251.

——, 1984: Abyssal eddy kinetic energy in the North Atlantic. *J. Mar. Res.*, **42,** 509–536.

——, and J. R. Luyten, 1990: Spectral time scales for mid-latitude eddies. *J. Mar. Res.*, **49,** 75–107.

Schultz, J. R., 1987: Structure and propagation of topographic Rossby waves northeast of Cape Hatteras, North Carolina. M.S. thesis. University of North Carolina. 44 pp.

Tai, C-K, and W. B. White, 1990: Eddy variability in the Kuroshio Extension as revealed by satellite altimetry: Energy propagation away from the jet, Reynolds stress, and seasonal cycle. *J. Phys. Oceanogr.*, **20,** 1761–1777.

Thompson, R., 1977: Observations of Rossby waves near Site D. *Progress in Oceanography,* Vol. 7, Pergamon, 135–162.

Thompson, R. O. R. Y., and J. R. Luyten, 1976: Evidence for bottom-trapped topographic Rossby waves from single moorings. *Deep-Sea Res.*, **23,** 629–635.

Watts, D. R., and W. E. Johns, 1982: Gulf Stream meanders: Observations on propagation and growth. *J. Geophys. Res.*, **87,** 9467–9476.

Welsh, E. B., N. G. Hogg, and R. M. Hendry, 1991: The relationship of low-frequency variability near the HEBBLE Site to Gulf Stream fluctuations. *Mar. Geol.*, **99,** 303–317.